ECMWF COPERNICUS REPORT

Copernicus Climate Change Service

Algorithm Theoretical Basis Document

Sea Ice Thickness – CryoSat-2/SMOS, Version 1.0

Issued by: Alfred Wegener Institute / Stefan Hendricks
Date: 24/02/2023
Ref: WP2-FDDP-2022-09_C3S2-Lot3_ATBD-of-v1.0-SeaIceThickness-CS2SMOS-product_v1.1
Official reference number service contract: 2021/C3S2_312a_Lot3_METNorway/SC1

Please cite as: Hendricks, S., Ricker, R., Kaleschke, L., Tian-Kunze, X. (2023) Sea Ice Thickness – CryoSat-2/SMOS Version 1.0: Algorithm Theoretical Basis Document. Copernicus Climate Change Service, Document reference: WP2-FDDP-2022-09_C3S2-Lot3_ATBD-of-v1.0-SeaIceThickness-CS2SMOS-product_v1.1.

This document has been produced in the context of the Copernicus Climate Change Service (C3S).
The activities leading to these results have been contracted by the European Centre for Medium-Range Weather Forecasts, operator of C3S on behalf on the European Union (Contribution Agreement signed on 22/07/2021). All information in this document is provided "as is" and no guarantee of warranty is given that the information is fit for any particular purpose.
The users thereof use the information at their sole risk and liability. For the avoidance of all doubt, the European Commission and the European Centre for Medium-Range Weather Forecasts have no liability in respect of this document, which is merely representing the author's view.

Contributors

ALFRED WEGENER INSTITUTE
Stefan Hendricks
Robert Ricker
Lars Kaleschke
Xiangshan Tian-Kunze

History of modifications

Version	Date	Description of modification	Chapters / Sections
v1.0	12/12/2022	Initial Version	All
v1.1	24/02/2023	Document amended to account for independent review suggestions, and finalized for publication	All

List of datasets covered by this document

Deliverable ID	Product title	Product type (CDR, ICDR, REP, OREP)	Version number	Delivery date
WP2-FDDP-2022-09	Reprocessed Northern Hemisphere Sea Ice Thickness from merged CryoSat-2/SMOS data	REP[1]	1.0	01/10/2022
WP2-ICDR-SIT-CS2SMOS-v1.0	Operationally Reprocessed Northern Hemisphere Sea Ice Thickness from merged CryoSat-2/SMOS data	OREP[1]	1.0	28/02/2023 to present

Related documents

[1] The limited temporal coverage of the CS2SMOS dataset does not allow for them to be classified as CDR or ICDR categories, as is typically done for other C3S datasets. This is why the “reprocessed dataset” (REP) and “operational reprocessed dataset” (OREP) are used here instead. The OREP corresponds to the temporal extension of the REP with timely updates.

Reference ID	Document
D1	Hendricks S. et al. (2022) SMOS/CryoSat-2 L4 Ice Thickness ATBD v2.4, ESA SMOS ESL for Geophysical (L3 & 4) data over land ice and sea ice. Technical Report delivered under ESA Contract No. ARG-003-081/SMOS-2020/AWI.
D2	Tian-Kunze et al. (2021) SMOS L3 Ice Thickness ATBD v1, ESA SMOS ESL for Geophysical (L3 & 4) data over land ice and sea ice
D3	Hendricks, S. et al. (2023) Sea Ice Thickness – CryoSat-2/SMOS Data Record Version 1.0: Product Quality Assessment Report. Copernicus Climate Change Service, Document reference: WP2-FDDP-2022-09_C3S2-Lot3_SeaIceThickness-CS2SMOS-product_v1.x

Acronyms

Acronym	Definition
C3S	Copernicus Climate Change Service
CDR	Climate Data Record
CDS	Climate Data Store
CS2	CryoSat-2 – ESA Earth Explorer Mission
CS2SMOS	CryoSat-2/SMOS merged sea ice thickness product
EASE2	Equal-Area Scalable Earth Grid – version 2
ESL	Expert Support Lab
FTP	File Transfer Protocol
FYI	First-year sea ice
ICDR	Interim Climate Data Record
L2P	Level-2 pre-processed
MYI	Multi-year sea ice
NSIDC	National Snow and Ice Data Center
OSI SAF	Ocean and Sea Ice Satellite Application Facility
OI	Optimal Interpolation
RM-TN	Readme First – Technical Note
SAR	Synthetic Aperture Radar (CryoSat-2 radar mode)
SIN	SAR Interferometric (CryoSat-2 radar mode)
SIRAL	SAR Interferometric Radar Altimeter (CryoSat-2 main sensor)
SIT	Sea Ice Thickness
SMOS	Soil Moisture and Ocean Salinity – ESA Earth Explorer Mission

Table of Contents

Scope of the document

This document is the Algorithm Theoretical Basis Document (ATBD), which describes the scientific background, the source data, and the processing steps used for creating the reprocessed sea ice thickness data record from merged CryoSat-2 and SMOS sea ice thickness data, as well as the output variables. The document is derived from a precursor ATBD document [D1], developed under a European Space Agency contract (ESA Contract No. ARG-003-081/SMOS-2020/AWI).

Executive Summary

The Algorithm Theoretical Basis Document (ATBD) describes data fusion approach behind the CryoSat-2/SMOS sea ice thickness product. The document contains a description of the input data sets, the algorithm used for the data fusion and the output variables of the product files.

The reprocessed CryoSat-2/SMOS (CS2SMOS) data record provides gap-less sea ice thickness data with coverage of the northern hemisphere at a spatial resolution of 25 km. This is achieved by optimal interpolation of CryoSat-2 and SMOS sea ice thickness source data with a temporal coverage of 7 days each. Both source datasets have complementary sensitivity to different thickness classes: SMOS for thin ice of 1 meter or less, and CryoSat-2 for the full range albeit at significantly higher relative uncertainty below 1 meter. The dataset collection is updated daily between October 18 and April 12 with reprocessed CryoSat-2 and SMOS datasets.

This dataset enables the computation of sea ice volume, but note that is not categorized as a climate data record due to the limited temporal coverage from November 2010 to the present day. The optimal interpolation approach yields a smoother representation of sea ice thickness than the C3S SIT CDR/ICDR, which does not rely on spatial averaging beyond grid cell resolution. The uncertainty of CS2SMOS data is 0.35 m.

The CS2SMOS data is generated by the ESA CryoSat-2/SMOS production and dissemination service (CS2SMOS-PDS) and further algorithm development is supported by the SMOS ESL sea ice project. Format and content of the CS2SMOS data is adapted for C3S/CDS data standards.

Overview of version evolution

This document is the first version describing the initial algorithm of the reprocessed CryoSat-2/SMOS merged sea ice thickness dataset version 1.0. This algorithm version corresponds to v2.05 of the ESA SMOS - CryoSat L4 Sea Ice Thickness data product[2], which is the basis for the data record described in this document.

[2] https://earth.esa.int/eogateway/catalog/smos-cryosat-l4-sea-ice-thickness (Last accessed December 2022)

1. Instruments

1.1 SMOS Data

The Soil Moisture and Ocean Salinity (SMOS) mission carries the Microwave Imaging Radiometer using Aperture Synthesis (MIRAS), a sensor for passive microwave remote sensing of the Earth surface at 1.4 GHz (L-Band). In addition to the named objectives of measuring soil moisture and ocean salinity, MIRAS data can be used to determine the thickness of sea ice in the thinner fraction of the sea ice thickness distribution, using the full-polarimetric MIRAS data.

Table 1: Properties of MIRAS instrument onboard SMOS.

Property	**Description**
Main Nominal Frequency	L-Band, 1.4 GHz, 21 cm
Type	passive microwave 2-D interferometric radiometer
Spatial Sampling	resampled to 15 km grid
Footprint	33 - 50 km depending on the position in the swath

1.2 CryoSat-2 Data

CryoSat's primary instrument is the Synthetic Aperture Interferometric Radar Altimeter (SIRAL), a Doppler-delay radar altimeter optimized for the estimation of ice sheet elevation and sea ice freeboard. SIRAL uses along-track synthetic aperture radar processing to improve the elevation resolution in flight direction. The radar operates in different modes depending on a predefined region mask. The two modes SAR (synthetic aperture radar) and SIN (interferometric SAR) are relevant for measurements over sea ice covered ocean and a regional mask governs their activation.

Table 2: Properties of CryoSat's SIRAL instrument.

Property	**Description**
Main Nominal Frequency	13.575 GHz
Radar Type	Delay-Doppler
Height Resolution	23 cm
Spatial Sampling	Approx. 300 m
Footprint	300 m x 1600 m (along x across track)
Orbit Inclination	92.00°

2. Input and auxiliary data

2.1 Primary Data

Primary datasets for CS2SMOS SIT are the individual SIT products derived from CryoSat-2 and SMOS respectively.

2.1.1 CryoSat-2

The source for CS2 SIT input data is the Level-2 pre-processed (L2P) data product[3] of the Alfred Wegener Institute in version 2.5 (described in Hendricks and Paul, 2022). The files with a daily resolution contain a summary of all SIT retrievals at full sensor resolution from CryoSat-2 orbits for a UTC calendar day, and also include an uncertainty estimate.

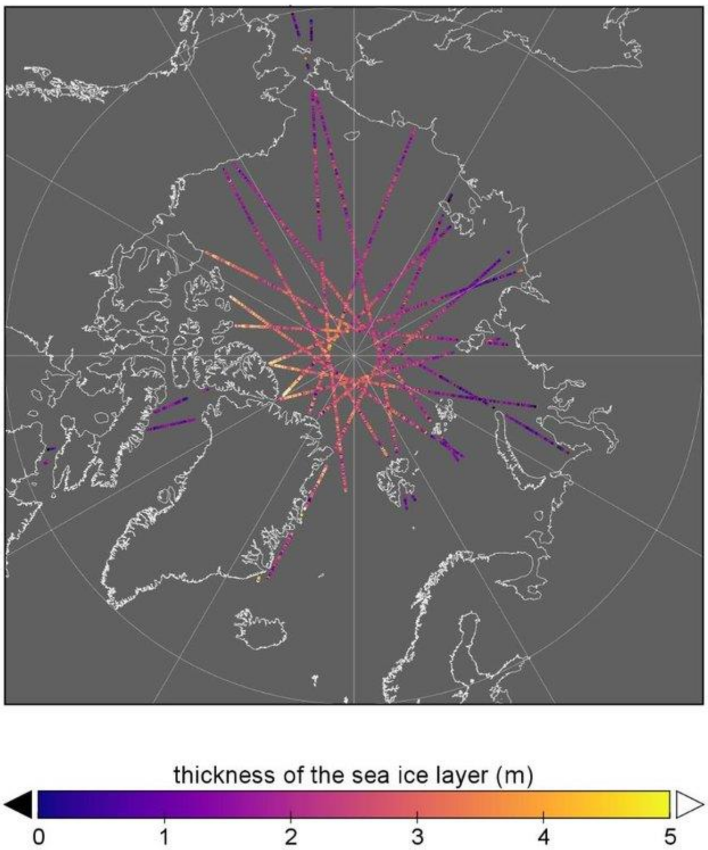

Figure 1: Example of CryoSat-2 l2p data consisting of all SIT information derived from all CS2 orbits for a UTC Day, at full CS2 sensor resolution.

[3] See the AWI CryoSat-2 project website: https://spaces.awi.de/display/SIRAL/ (Last accessed: December 2022)

The CS2 L2P data is based on reprocessed CS2 L1B data of the official ESA ICE baseline-D and baseline-E instrument processing facility. CS2 L1B data is ingested with a delay of 31 days and produced each northern winter season between Oct. 1 and April 30. A full description of the CryoSat-2 sea ice thickness retrieval, which is analogous to the C3S SIT CDR/ICDR is given in Hendricks and Paul, 2022.

Table 3: Overview of CryoSat-2 sea ice thickness source data.

Product	Source	Frequency	Spatial coverage	Resolution
CS2 sea ice thickness L2P v2.5	ftp://ftp.awi.de/sea_ice[4]	Daily	Daily Orbits	300 m x 1600 m (along x across track)

2.1.2 SMOS

The source for SMOS SIT input data are daily gridded ESA SMOS Sea Ice Thickness Product v3.3 on a polar-stereographic grid with a resolution of 12.5 km (Tian-Kunze et al., 2014). Each product contains SIT information up to 1.0 m. SMOS sea ice thickness is generated from October 15 to April 15 for each Arctic winter season since 2010.

Table 4: Overview of SMOS sea ice thickness source data.

Product	Source	Frequency	Spatial coverage	Grid/ resolution
SMOS sea ice thickness L3C v3.3	ftp://ftp.awi.de/sea_ice[4]	Daily	Entire Arctic	Polarstereo 12.5 km (EPSG:3411)

A full description of the SMOS sea ice thickness retrieval is given in [D2]. Information on the SMOS product is available on the website of the SMOS & CryoSat-2 Sea Ice Data Product Processing and Dissemination Service (CS2SMOS-PDS)[5].

[4] Last accessed February 20th, 2023. Requires FTP client (e.g., FileZilla) or FTP capable file explorer to open

[5] https://spaces.awi.de/display/CS2SMOS (Last accessed December 2022).

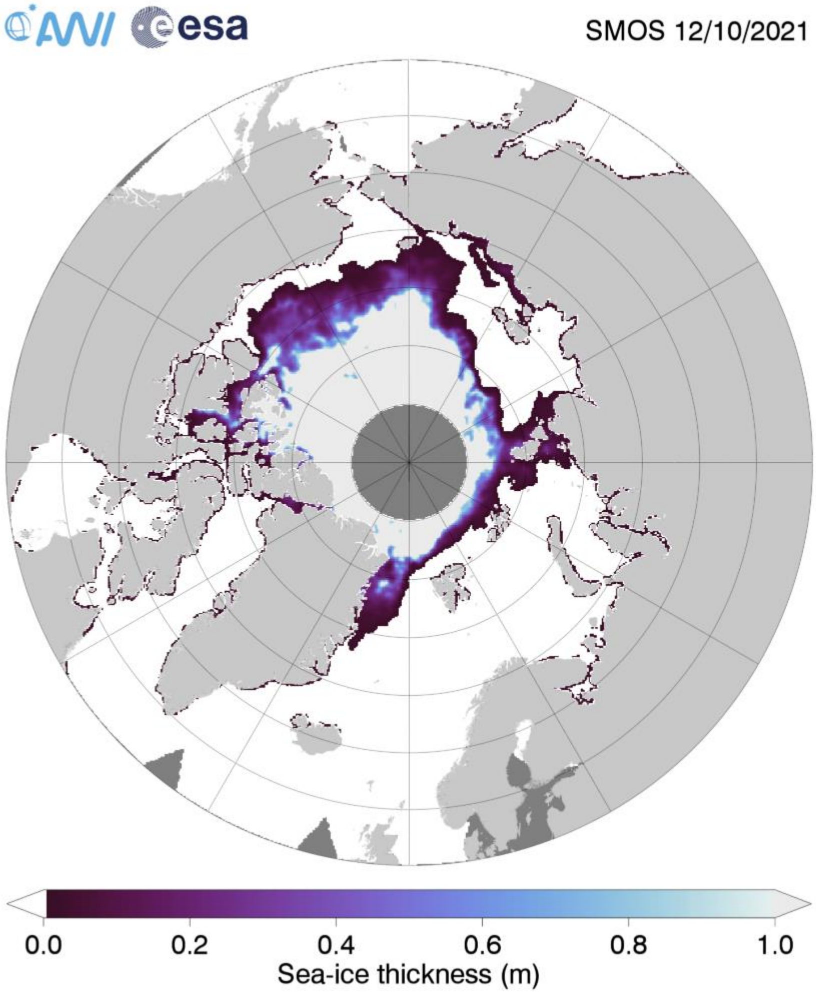

Figure 2: Example of daily SMOS sea ice thickness grid. Source: ESA SMOS L3C product version 3.3 with thickness data between 0 and 1.0 m.

2.2 Auxiliary Data

Auxiliary information is needed for the reference sea ice mask, provided by sea ice concentration, as well as for masking SMOS data in multi-year ice areas, provided by sea ice type information. In addition, an ocean/land mask is used in the algorithm.

Table 5: Overview of auxiliary data used for the CryoSat-2/SMOS data fusion

Product	Source	Frequency	Spatial coverage	Grid/ resolution
OSI-SAF sea ice concentration CDR/ICDR v2.0	ftp://osisaf.met.no/ reprocessed/ice/conc-cont-reproc/v2p0/[6]	Daily	Entire Arctic	EASE2 grid 25 km (EPSG:6931)
OSI-SAF operational sea Ice type (OSI-403-c)	ftp://osisaf.met.no/ archive/ice/type/[7]	Daily	Entire Arctic	Polarstereo 10 km
Ocean/land mask	ftp://osisaf.met.no/ reprocessed/ice/ oceanmasks/[7]	Static	Entire Arctic	

[6]Last accessed February 20th, 2023. Requires FTP client (e.g., FileZilla) or FTP capable file explorer

3. Algorithm

3.1 Overview

3.1.1 Objective

The main objective of the CryoSat-2/SMOS data merging is to ensure that sea ice thickness product users can benefit from the two sensors different, but complementary, sensitivities towards different ice thickness categories. The Soil Moisture and Ocean Salinity (SMOS) mission provides L-band observations, and the ice thickness-dependency of brightness temperature enables the estimation of sea-ice thickness for thin ice regimes, during the freeze-up (Kaleschke et al., 2012). On the other hand, CS2 uses radar altimetry to measure the height of the ice surface above the water level, which can be converted into sea-ice thickness assuming hydrostatic equilibrium. In contrast to SMOS, The CS2 mission was primarily designed to measure the thickness of the perennial and thick first-year ice cover and lacks the sensitivity for thin ice regimes (Wingham et al., 2006).

The complementary nature of the relative uncertainties of CS2 and SMOS ice thickness retrievals has been shown by Kaleschke et al. (2015). **Figure 3** illustrates uncertainty maps and the relative uncertainties of CS2 and SMOS monthly means from March 2016. While the SMOS relative uncertainties are lowest for very thin ice, CS2 relative thickness uncertainties are smaller over thick ice, and rise asymptotically towards thickness values < 1 m.

Also, the spatial coverage is of a complementary nature due to the different orbital inclinations. **Figure 4** shows weekly means of CS2 and SMOS during the freezing season 2015/16. While valid SMOS ice thickness estimates can be found mostly in the marginal ice zones, the CS2 ice thickness retrieval covers major parts of the Arctic multiyear ice (MYI). **Figure 5** illustrates the number of sea ice thickness observations of either CryoSat-2, SMOS or both for 7-day periods over one winter season. Only a minority of grid cells are covered by both CryoSat-2 and SMOS observations.

Therefore, merging of CS2 and SMOS sea-ice thickness retrievals has the capability to provide a better view of the Arctic sea-ice thickness distributions. However, note that gap filling by interpolation is also necessary to provide sea ice thickness information for the entire sea ice cover with CryoSat-2 and SMOS data from 7 days (**Figure 5**).

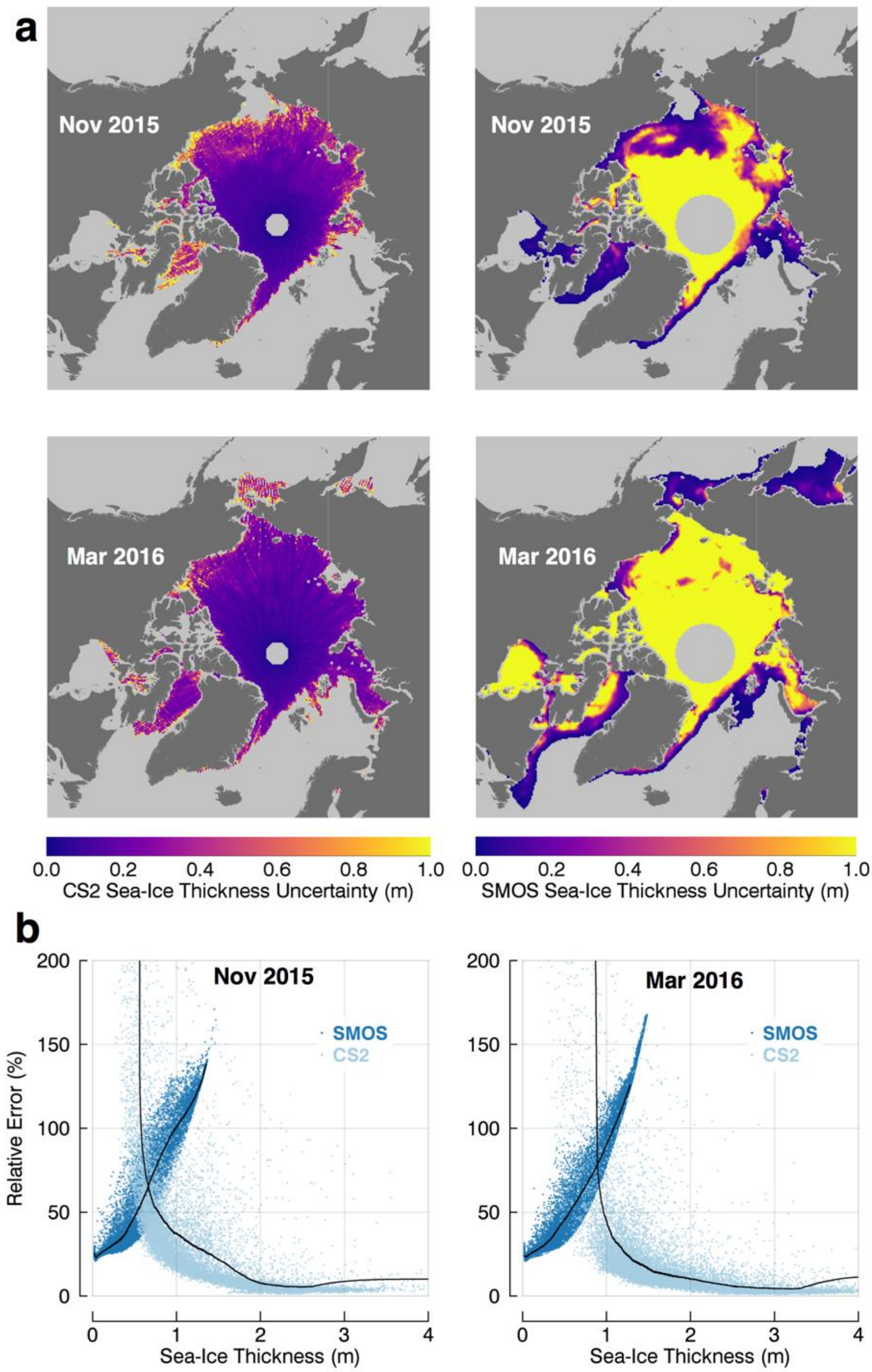

Figure 3: Uncertainty maps and the relative uncertainties of CS2 and SMOS monthly means. a) Monthly sea-ice thickness uncertainty maps of the CryoSat-2 (left panels) and SMOS (right panels) retrieval from November 2015 and March 2016. b) Relative uncertainties from November 2015 and March 2016 for the two sensors presented together. A running mean is represented by black solid lines.

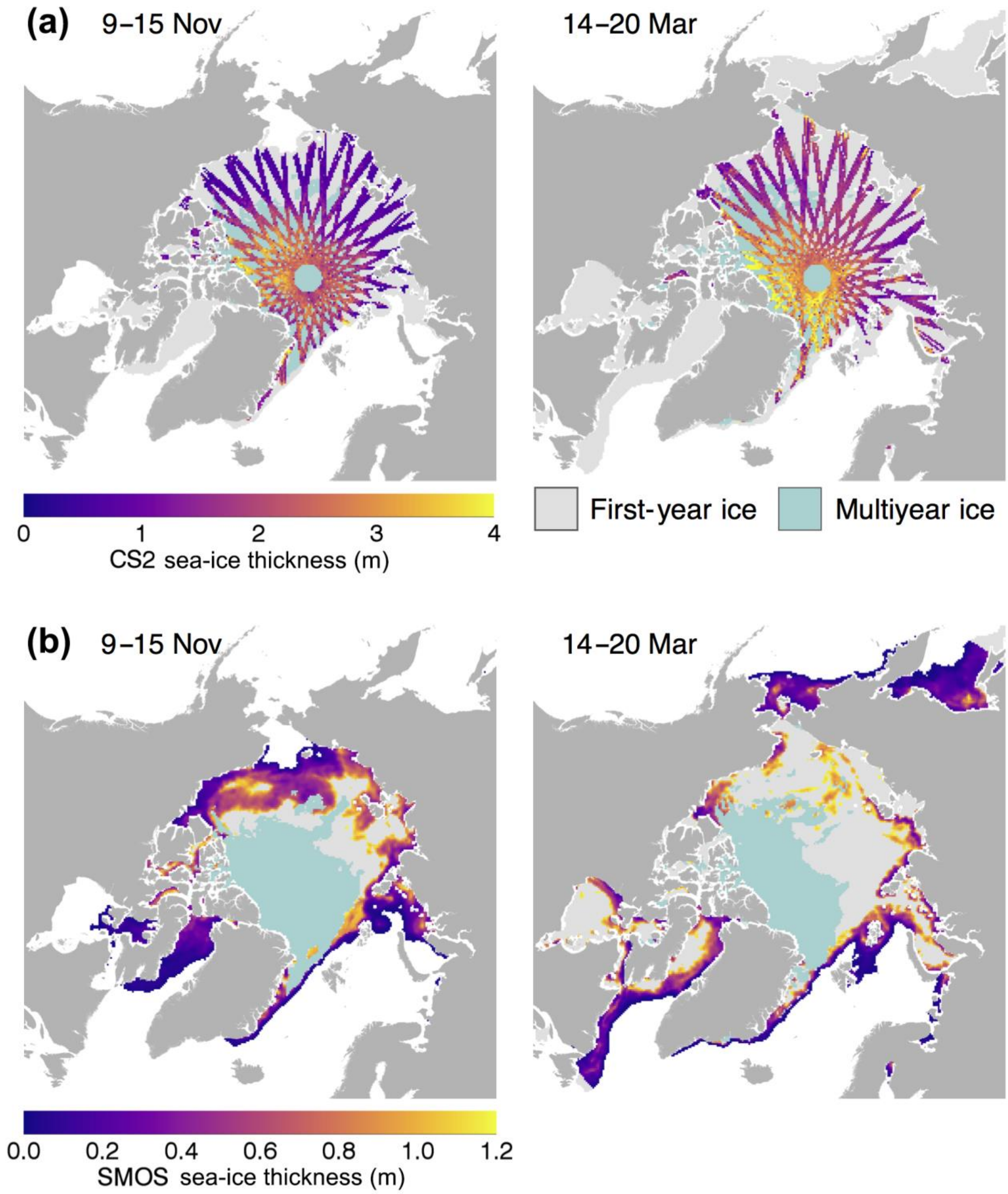

Figure 4: Averaged data grids for 7-day periods at the beginning and end of the Arctic winter season 2015/16. a) CryoSat-2 retrieval as used for the optimal interpolation. b) 7 day means of daily SMOS ice thickness retrievals, cropped by a 1 m maximum SMOS thickness uncertainty (Figure from Ricker et al, 2017; The Cryosphere)

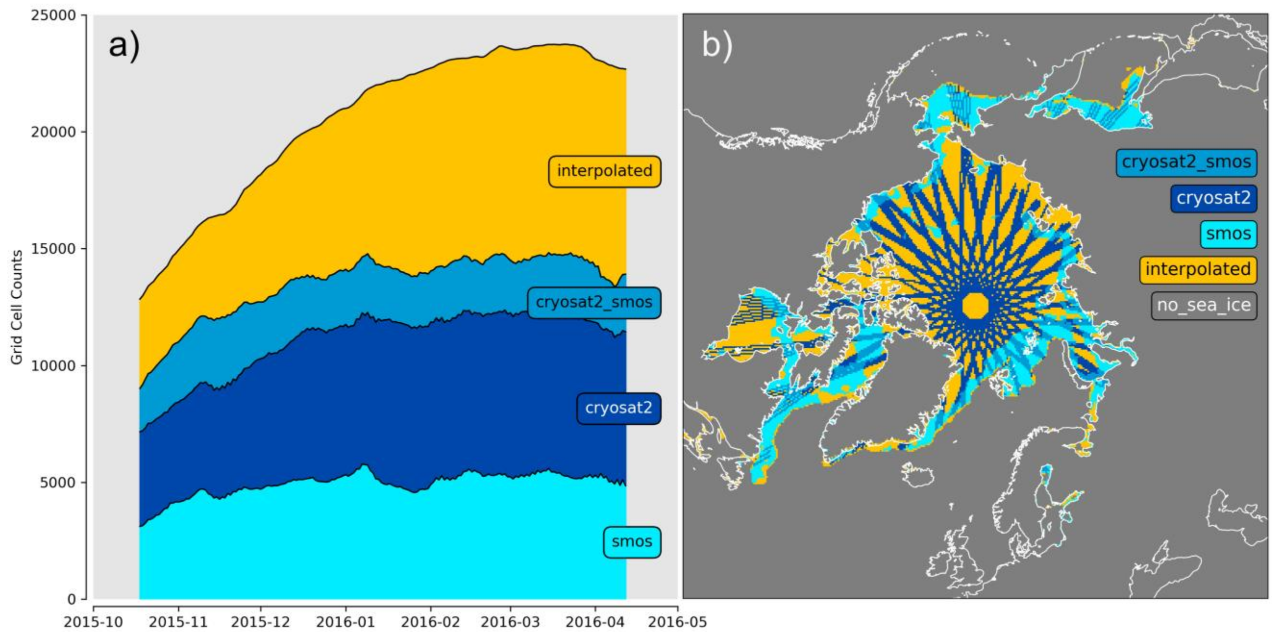

Figure 5: a) Spatial coverage in number of valid 25 km grid cells from October 2015 to April 2016. Counted are grid cells that contain only SMOS (smos), only CryoSat-2 (cryosat2), both (cryosat2_smos) or none and are based on interpolation (interpolated). b) Regional distribution of the grid cell covered by either SMOS, CryoSat-2, both or where sea ice thickness is fully based on interpolation.

3.1.2 Data Fusion Approach

We use an optimal interpolation (OI) scheme akin to those described in Böhme and Send (2005), Boehme et al. (2008), and McIntosh (1990), that allows the merging of datasets from diverse sources on a predefined analysis grid. The data are weighted differently based on known uncertainties of the individual products and modeled spatial covariances. OI minimizes the total error of observations and provides ideal weighting for the observations at each grid cell. The data merging methods were first described in Ricker et al. (2017). Here, we present the processing methods, on which optimal interpolation is based. Figure 6 shows the processing scheme which is described in more detail in the following sections.

The OI scheme is used to get an objective estimate of values at observed or unobserved locations.

The basic equation is:

$$Z_a = Z_b + \mathbf{K}[Z_o - H(Z_b)], \qquad (1)$$

with the vector Z_a is the analysis field that represents the merged CS2SMOS ice thickness retrieval which we aim for. Z_b is the background field vector and Z_o the vector that contains all SMOS and CS2 observations. **K** is a weight matrix. As observations we here define already gridded thickness estimates, based on aggregated data of 7 days. This approach reduces statistical uncertainties and provides equally distributed observations, which improves the performance of the OI. In addition, it is reasonable to reduce the number of observations, otherwise computing can become time-consuming. We assume that the observations are static, which is a simplification, because the satellite thickness estimates are temporally incoherent due to ice deformation and motion. Therefore, we neglect any temporal correlations. H is an operator that transforms the background field into the observation space. This is achieved by an inverse distance interpolation method.

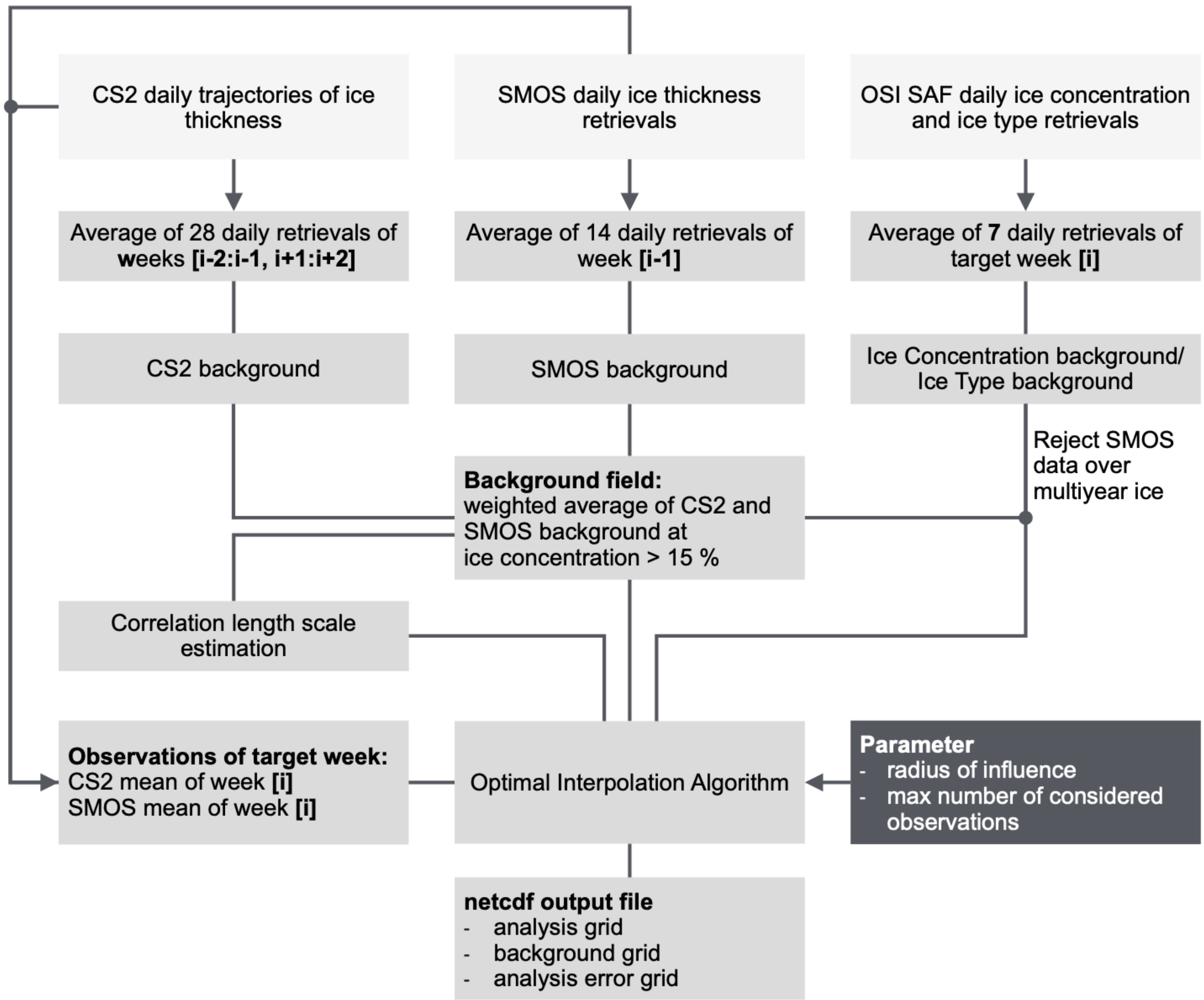

Figure 6: Workflow showing the processing chain that implements CryoSat-2/SMOS data merging.

3.1.3 Temporal Coverage and Resolution

Temporal aggregation of CryoSat-2 data is needed for the optimal interpolation to overcome the sparseness of altimeter-based SIT information on a single day. The input observation for the optimal interpolation may have gaps, but the background fields need to be without gaps. Therefore, a longer temporal data aggregation is required for Z_b than Z_o. Figure **7**7 illustrates the temporal coverage and resolution of the observations and background field.

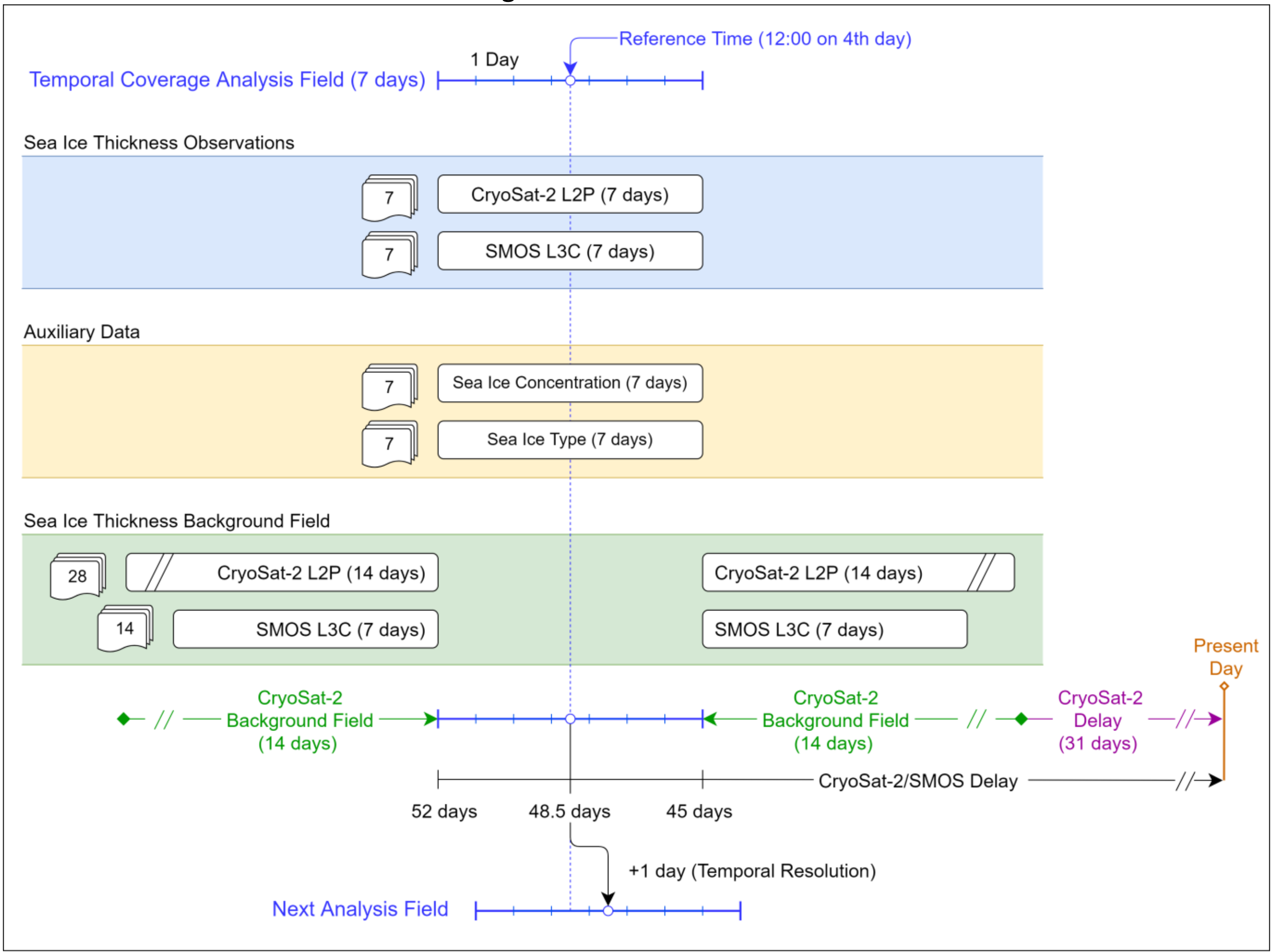

Figure 7: Temporal coverage, resolution, and delay of the CryoSat-2/SMOS analysis fields as well as the auxiliary data and background field.

The observations, and thus the analysis field have a temporal coverage of 7 days. CS2 data for the background field consists of 28 days, and SMOS data of 14 days. The background field should be independent from the observations and centered around the reference time, to avoid introducing a phasing bias. The CS2 (SMOS) background field therefore contains 14 (7) days before the start and 14 (7) days after the end of the observation period, which results in 35 (21) days of sea ice thickness data needed for one CS2SMOS product file.

The requirement of 35 days of CS2 SIT data for the background and observation field determines the delay of the CS2SMOS production with respect to the current day. The input CS2 data is available with a delay of 31 days, thus the background field requirement allows an observation period that is delayed from 52 to 34 days with respect to the current day.

While CS2 data availability determines the delay of CS2SMOS, SMOS data availability determines the temporal coverage in each winter season. Daily SMOS sea ice thickness data is only generated between October 15 and April 15 and these dates define the limits for the observation period. The first product reference time in each winter is October 18, while the last is April 12. The decision to use the full SMOS data period for the observation field means that in the first and last week the SMOS background field is incomplete. This is a deliberate compromise between accuracy and temporal coverage.

3.2 Background Field

We use daily trajectories (L2P) of sea ice thickness from CS2 that are collected for the required periods (Section 3.1.3) and grid the data to the target grid (Section 4.1). The initial background field is represented by a weighted average:

$$\overline{Z} = \frac{Z_{cs2}/\sigma^2_{cs2} + Z_{smos}/\sigma^2_{smos}}{1/\sigma^2_{cs2} + 1/\sigma^2_{smos}} \tag{2}$$

Z is the sea-ice thickness and σ the statistical uncertainty of the individual products. In addition, we use an ice concentration mask, based on 7 days of the OSI SAF sea ice concentration product, to determine the ice coverage during the target week. The ice concentration mask is needed to limit CS2 and SMOS retrievals for the background field to the ice coverage of the target week, and to mask SMOS artifacts of thin ice (< 10 cm) in coastal regions that may be caused by land signal spill over. Here, a threshold of 15 % is applied to the 7-day sea ice concentration mean, and only grid cells that exceed this value are to be considered as ice covered. This corresponds to the ice extent products provided by OSI SAF and the National Snow and Ice Data Center (NSIDC). Gaps in the weighted average, derived from Eq. 2, are interpolated by using a nearest neighbor scheme. Before it is applied in the optimal interpolation algorithm, the background field is low pass filtered to reduce noise. An unfiltered version of the background field is kept for the next step.

3.3 Correlation Length Scale

The correlation length scale ξ controls the impact of a data point on the analysis grid point depending on the distance. Considering the grid resolution of 25 km, we aim for large scale correlations. Ideally, our correlation length scale estimate is large in the center of a certain ice type regime with similar ice thickness (i.e., level first-year sea ice (FYI)). On the other hand, we expect a low ξ value at locations with varying thickness gradients. **Figure 8** illustrates the estimation of ξ for a certain grid cell Z_0 in the Lincoln Sea during a week in November. To estimate ξ, we consider the unfiltered background field Z_b (**Figure 8**a). In the following, we define a structure function ϵ^2, which is related to the normalized auto correlation function $R(d, Q)$ as follows (Böhme & Send, 2005):

$$\epsilon^2(\mathrm{d},\mathrm{Q}) = \overline{\left(Z'_0 - Z'_{Q,d}\right)^2} = 2\,\overline{\sigma^2_{Z'}} - 2\,\overline{\sigma^2_{Z'}}\mathrm{R}(\mathrm{d},\mathrm{Q}) \tag{3}$$

$$R(d,Q) = 1 - \frac{\epsilon^2(d,Q)}{\overline{2\sigma^2_{Z'}}} \tag{4}$$

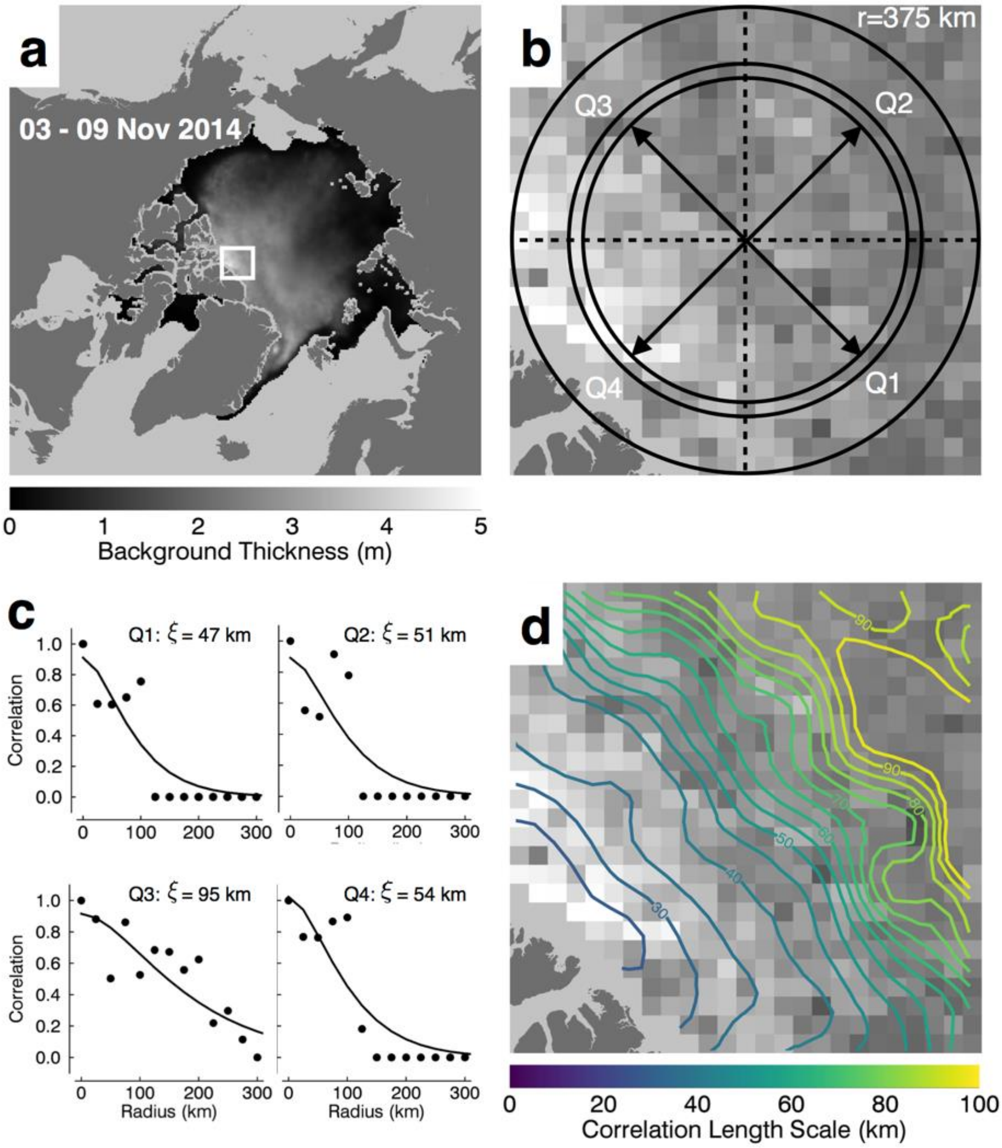

Figure 8: Scheme for the estimation of the correlation length scale ξ for a single grid cell for the target week 3-9 November 2014. a) Background field with indicated area of interest (white box). b) Adjacent ice thickness grid cells within a radius of 375 km are binned into annuli of distance and 4 quadrants. (c) Binned thickness estimates are used to calculate the structure function of each quadrant. ξ is estimated by fitting an exponential function. d) Contour map of estimated correlation length scales for the considered area.

Quadrants Q are defined to accommodate the anisotropy of the spatial ice thickness distribution (**Figure 8**b). $\epsilon^2(d, Q)$ represents the squared differences between ice thickness of the grid cell and the ice thickness of the grid cells of binned 25 km distances d in a quadrant Q. $Z'_{Q,d}$ is the unfiltered background thickness, binned according to d and Q. Figure 8b reveals the annuli of distance and the 4 Quadrants. $\sigma^2_{Z'}$ are the corresponding mean variances of a certain quadrant.

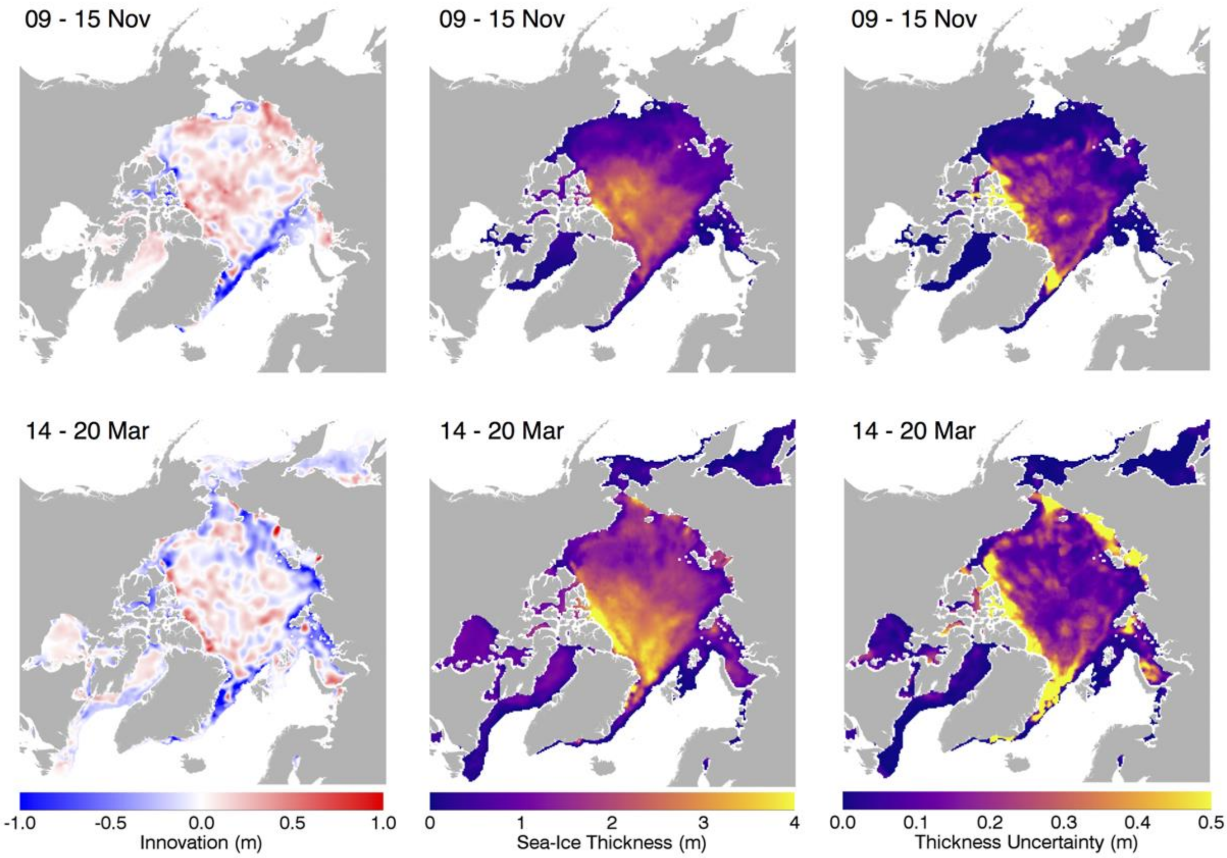

Figure 9: Output grids from the optimal interpolation processing for weeks in November 2015 and March 2016: The innovation (left column) is the difference between background and the merged product ice thickness (center column). The sea-ice thickness uncertainty of the optimal interpolation product is derived from the relative analysis error, scaled with the observation variances (right column).

With Eq. 4, we then obtain the auto correlation function $\mathrm{R}(\mathrm{d}, \mathrm{Q})$, which is computed up to a radius of 750 km (30 bins). In the next step, we fit a function $R(d, Q)$ of the form:

$$C(d, \xi) = \left(1 + \frac{\mathrm{d}}{\xi}\right) \exp\left(\frac{-\mathrm{d}}{\xi}\right) \tag{5}$$

with a non-linear least squares approach and obtain an estimate for ξ. Figure 8c shows the calculated auto correlation function $R(d, Q)$ and the functional fit (Eq. 5). A stronger decay of $R(d, Q)$ occurs with rising deviation between Z_0 and the thickness at a certain distance in a certain quadrant. $R(d, Q)$ can also become negative if $\epsilon^2(\mathrm{d}, \mathrm{Q}) \;/\; \overline{2\sigma_Z^2}$, becomes >1. To improve the fitting performance, we set $R(d, Q) \;=\; 0$ if $R(d, Q)$ becomes < 0. Furthermore, ξ is rejected if the computation fails. Finally, we average the ξ values from the 4 quadrants. To remove outliers and noise, the derived ξ grid is low pass filtered with a smoothing radius of 25 km (see section 4.1 for grid definition). Grid cells with failed computation are interpolated by a nearest neighbor scheme afterwards. Figure 8d shows the spatial correlation length scales ξ for 3-9 November 2014. It highlights the sensitivity to changing thickness gradients as ξ decreases towards the coast of the Canadian Archipelago, where higher sea ice thickness gradients likely occur due to increased deformation.

3.4 Optimal Interpolation

The weight matrix **K**, which is needed for the computation of Z_a, is retrieved by the background error covariance matrix **B** in the observation space, multiplied by the inverted total error covariance matrix:

$$K=BH^T\left(R + HBH^T\right)^{-1}, \tag{6}$$

where **R** is the error covariance matrix of the observations. To reduce computation expense, we assume the following:

1. We neglect correlations of observation errors which means that **R** is a matrix with non-zero elements only on the diagonal. These variances are represented by the SMOS and CS2 product uncertainties.
2. We assume that the influence of observations that are located far away from the analysis grid point can be neglected. Therefore, instead of computing the entire covariance matrix, we only consider observations within a radius of influence. This radius is set to 250 km to gather just enough observations in regions with large gaps, for example over MYI between two CS2 orbits where valid SMOS observations are not available.
3. We limit the number of matched observations to 120, to further reduce computation expense. This means that in the case of more matches, only the 120 closest observations are considered.
4. We generally assume that all observations are unbiased.

$\mathbf{bh}^{\mathrm{T}}$ and $\mathbf{hbh}^{\mathrm{T}}$ are estimated using the correlation function in Eq. 5:

$$(bh^T)_i = \left(1 + \frac{d\left(x_{o_i}, x_{a_{m,n}}\right)}{\xi_{m,n}}\right) exp\left(\frac{-d\left(x_{o_i}, x_{a_{m,n}}\right)}{\xi_{m,n}}\right) \tag{7a}$$

$$(hbh^T)_{i,j} = \left(1 + \frac{d\left(x_{o_i}, x_{o_j}\right)}{\xi_{m,n}}\right) exp\left(\frac{-d\left(x_{o_i}, x_{o_j}\right)}{\xi_{m,n}}\right) \tag{7b}$$

$$d(x, y) = \|x - y\| \tag{8}$$

Here, x_{o_i} and $\mathrm{x}_{\mathrm{o_j}}$ represent the locations of the matched observations within the radius of influence. $x_{a_{m,n}}$ refers to the location of the analysis grid cell. Because of Eq. 7b, the impact of a data point decreases with increasing distance. The estimation of the correlation length scale ξ is described in section 3.3.

Computing $\mathbf{bh}^{\mathrm{T}}$ and $\mathbf{hbh}^{\mathrm{T}}$ allows the computation of the weight matrix **K**. Thus, we retrieve the second part of Eq. 1, which is called *innovation*. This iterative procedure is accomplished for each analysis grid cell, leading to the complete analysis grid $\mathrm{Z_a}$.

3.5 Analysis Error

The corresponding analysis error covariances are derived by:

$$\sigma_{Z_a}^2 = (\mathbf{I} - \mathbf{KH})\,\mathbf{B} \qquad (9)$$

Since we consider variances exclusively, we only calculate the diagonal elements of $\sigma_{Z_a}^2$. **Figure 9** shows the merged product and furthermore the innovation field and the analysis error, which is the root of the error variance. The analysis thickness uncertainty is a relative quantity ranging between 0 and 1, scaled with observation variances. It increases in gaps of CS2 data and where valid SMOS observations are not available, especially in the Canadian Archipelago or in the thick multi-year ice (MYI) zone of Fram Strait (**Figure 10**). In this case the analysis heavily depends on the background field, and therefore the SIT error increases. For validation of the merged product, we refer to Ricker et al. (2017), and the Readme First Technical Note (RM-TN)[7] in addition to [D3].

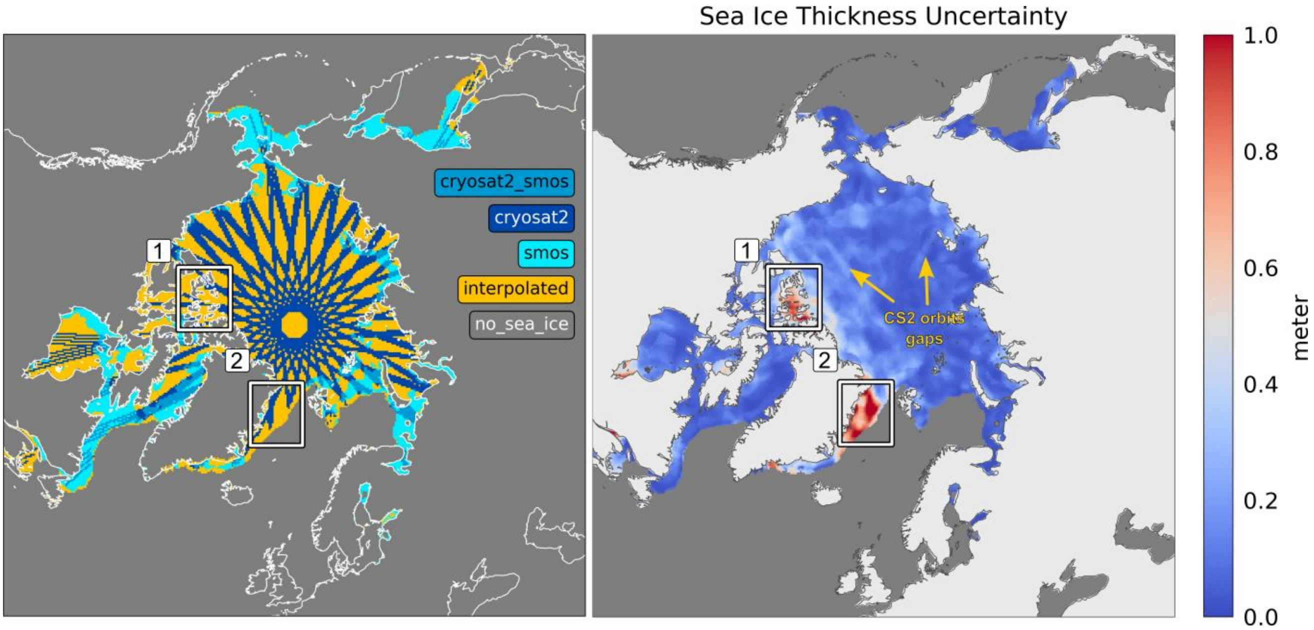

Figure 10: Sea ice thickness uncertainty as a function of CryoSat-2 and SMOS data coverage (marked as \`interpolated\` in left panel). Regions (1) and (2) feature low data coverage with resulting high uncertainties. The striping pattern of the gaps in the CryoSat-2 data coverage (marked as \`interpolated\` in left panel) are also visible in the CS2SMOS sea ice thickness uncertainty (yellow arrows in right panel).

[7] CS2SMOS technical documents: https://earth.esa.int/eogateway/catalog/smos-cryosat-l4-sea-ice-thickness (last accessed: December 2022)

4. Output Data

Each output dataset includes gridded merged sea ice thickness data from CryoSat-2 and SMOS on a polar grid (section 4.1). One product file is generated for each 7-day observation period, which is associated to a single day in the file, defined by the date of the reference time (Section 3.1.3).

The output parameters are limited to the main geophysical variable, sea ice thickness, and its uncertainty. The information is accompanied by two flags, which provides information of the retrieval process and the CryoSat-2 and SMOS input data (Section 4.2).

4.1 Grid

All grids are projected onto the 25 km Equal-Area Scalable Earth grid of version 2 (EASE2), which is based on a polar aspect spherical Lambert azimuthal equal-area projection (Brodzik et al., 2012) and the WGS84 ellipsoid. The grid dimension is 5400 km x 5400 km, equal to a 432 x 432 grid. The grid is centered on the geographic Pole, meaning that the Pole is located at the intersection of center cells (Figure 10).

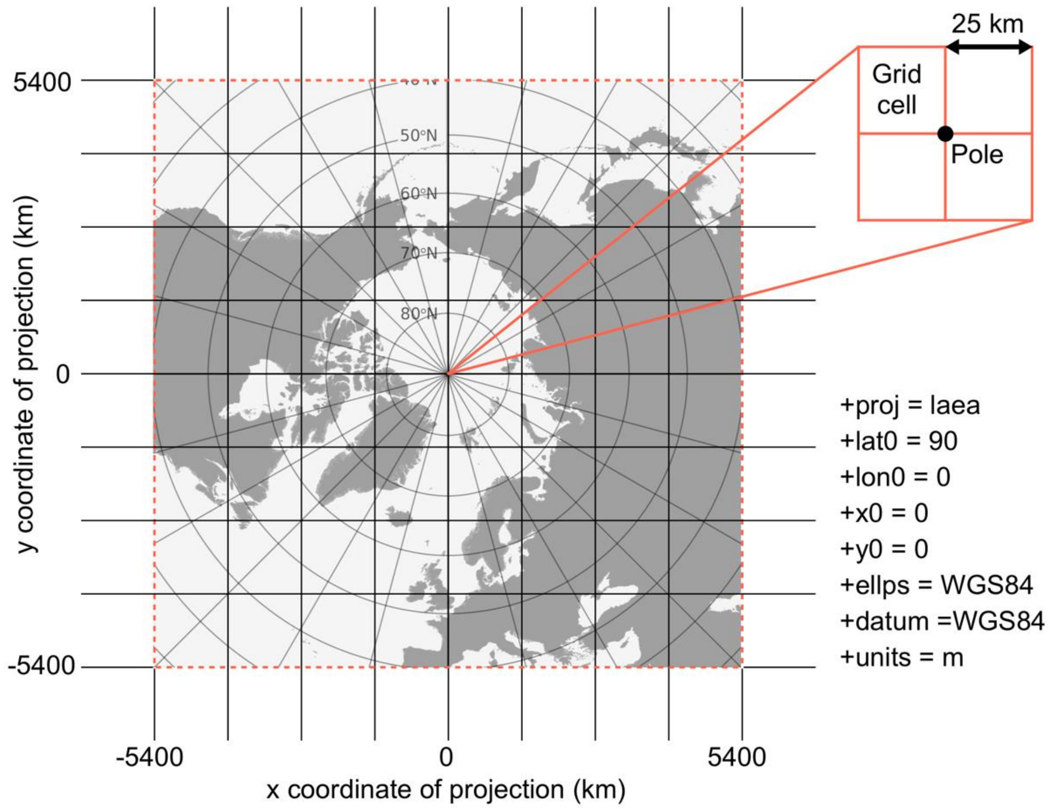

Figure 11: Specifications of the EASE2 25 km grid used for the CS2SMOS SIT v1.0 product.

4.2 Output Parameters

The output parameters, consist of gridded sea ice thickness, with associated uncertainty as well as status and quality flags. **Figure 12** illustrated the four parameters of the product file with for January 31, 2011 (ice_thickness_nh_ease2-250_cs2smos-v1p0_20110131.nc).

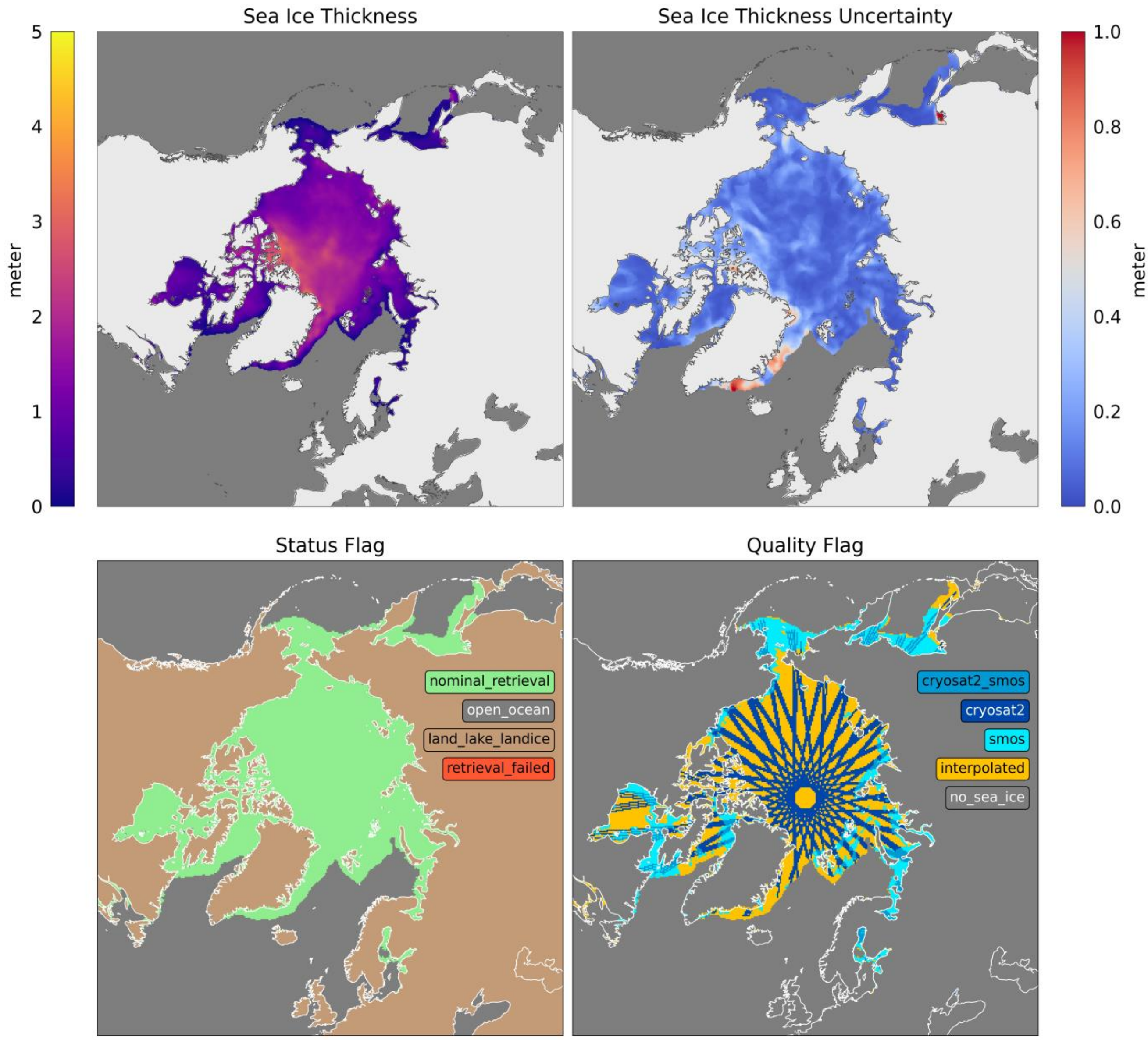

Figure 12: Output parameters in the CS2SMOS product files (example January 31, 2011). Upper left: sea ice thickness in meters, upper right: Sea ice thickness uncertainty in meters, lower left: status flag, lower right: quality flag. The flags are color coded by meaning of the flag provided by the `flag_meanings` variable attribute.

4.2.1 Sea Ice Thickness

The main geophysical parameter of the reprocessed CryoSat-2/SMOS data record. The value is defined as the mean thickness of the sea ice layer of the ice-covered fraction of the grid cell area.

Table 6: Variable attributes of sea ice thickness in product files.

Property	Value
Variable Name	`sea_ice_thickness`
Long Name	Sea Ice Thickness
Standard Name	`sea_ice_thickness`
Unit	`m`
Content	Thickness of the Analysis field (variable `analysis_sea_ice_thickness` in source CS2SMOS data)

4.2.2 Sea Ice Thickness Uncertainty

The uncertainty variable of the reprocessed CryoSat-2/SMOS data record computed as the product of analysis thickness and analysis error.

Table 7: Variable attributes of sea ice thickness uncertainty in product files.

Property	Value
Variable Name	`uncertainty`
Long Name	Sea Ice Thickness Uncertainty
Standard Name	`sea_ice_thickness standard_error`
Unit	`m`
Content	Based on analysis thickness and analysis error.

4.2.3 Status Flag

The status flag provides information on the sea ice and land masks and whether the retrieval was successful or not. The status flag is computed from analysis field, the sea ice concentration mask, and the land/sea mask.

Table 8: Variable attributes of status flag in product files.

Property	**Value**
Variable Name	`status_flag`
Long Name	Sea Ice Thickness Status Flag
Standard Name	`status_flag`
Unit	1

Content	`0: Nominal`
	`1: Open Ocean`
	`2: Land / Land Ice`
	`3: Retrieval Failed`

4.2.4 Quality Flag

The quality flag provides information of the source data per grid cell, and indicates which grid cells are populated by interpolation only. Grid cells with observations are likely to be more accurate than purely interpolated ones. The flags are computed from the availability of data in each grid cell and from the land/sea mask.

Table 9: Variable attributes of quality flag in product files.

Property	**Value**
Variable Name	`quality_flag`
Long Name	Sea Ice Thickness Quality Flag
Standard Name	`quality_flag`
Unit	1

Content	`0: CryoSat-2 & SMOS`
	`1: CryoSat-2`
	`2: SMOS`
	`3: Interpolated`
	`4: No Sea Ice`

References

Boehme, L., Meredith, M. P., Thorpe, S. E., Biuw, M., and Fedak, M.: Antarctic Cir- cumpolar Current frontal system in the South Atlantic: Monitoring using merged Argo and animal-borne sensor data, Journal of Geophysical Research: Oceans, 113, doi: 10.1029/2007JC004647, http://dx.doi.org/10.1029/2007JC004647, c09012, 2008.

Böhme, L. and Send, U.: Objective analyses of hydrographic data for referencing profiling float salinities in highly variable environments, Deep Sea Research Part II: Topical Studies in Oceanography, 52, 651–664, 2005.

Brodzik, M. J., Billingsley, B., Haran, T., Raup, B., and Savoie, M. H.: EASE-Grid 2.0: Incremental but Significant Improvements for Earth-Gridded Data Sets, ISPRS International Journal of Geo-Information, 1, 32–45, doi:10.3390/ijgi1010032, URL http://www.mdpi.com/2220-9964/1/1/32, 2012.

Stefan Hendricks, & Stephan Paul. Product User Guide & Algorithm Specification: AWI CryoSat-2 Sea Ice Thickness (version 2.5) (2.5). Zenodo. https://doi.org/10.5281/zenodo.7416200, 2022

Kaleschke, L., Tian-Kunze, X., Maaß, N., Mäkynen, M., and Dr- usch, M.: Sea ice thickness retrieval from SMOS brightness tem- peratures during the Arctic freeze-up period, Geophys. Res. Lett., 39, L05501, doi:10.1029/2012GL050916, 2012.

L. Kaleschke, X. Tian-Kunze, N. Maaß, R. Ricker, S. Hendricks and M. Drusch, "Improved retrieval of sea ice thickness from SMOS and CryoSat-2," 2015 IEEE International Geoscience and Remote Sensing Symposium (IGARSS), pp. 5232-5235, doi: 10.1109/IGARSS.2015.7327014, 2015

Kaleschke, L., Tian-Kunze, X., Maaß, N., Beitsch, A., Wernecke, A., Miernecki, M., Müller, G., Fock, B. H., Gierisch, A. M., Schlünzen, K. H., Pohlmann, T., Dobrynin, M., Hen- dricks, S., Asseng, J., Gerdes, R., Jochmann, P., Reimer, N., Holfort, J., Melsheimer, C., Heygster, G., Spreen, G., Gerland, S., King, J., Skou, N., Søbjærg, S. S., Haas, C., Richter, F., and Casal, T.: SMOS sea ice product: Operational application and validation in the Barents Sea marginal ice zone, Remote Sensing of Environment, 180, 264-273, http://dx.doi.org/10.1016/j.rse.2016.03.009, special Issue: ESA's Soil Moisture and Ocean Salinity Mission - Achievements and Applications, 2016.

McIntosh, P. C.: Oceanographic data interpolation: Objective analysis and splines, Journal of Geophysical Research: Oceans (1978–2012), 95, 13 529–13 541, 1990.

Ricker, R., Hendricks, S., Kaleschke, L., Tian-Kunze, X., King, J., Haas, C. (2017). A weekly Arctic sea-ice thickness data record from merged CryoSat-2 and SMOS satellite data. The Cryosphere, 11, 1607-1623.

Tian-Kunze, X., Kaleschke, L., Maaß, N., Mäkynen, M., Serra, N., Drusch, M., and Krumpen, T.: SMOS-derived thin sea ice thickness: algorithm baseline, product specifications and initial verification, The Cryosphere, 8, 997–1018, doi:10.5194/ tc-8-997-2014, URL http://www.the-cryosphere.net/8/997/2014/, 2014.

Wingham, D., Francis, C., Baker, S., Bouzinac, C., Brockley, D., Cullen, R., de Chateau-Thierry, P., Laxon, S., Mallow, U., Mavrocordatos, C., Phalippou, L., Ratier, G., Rey, L., Rostan, F., Viau, P., and Wallis, D.: CryoSat: A mission to determine the fluctuations in Earth's land and marine ice fields, Adv. Space Res., 37, 841–871, https://doi.org/10.1016/j.asr.2005.07.027, 2006.

ECMWF - Shinfield Park, Reading RG2 9AX, UK

Contact: https://support.ecmwf.int/